Supplementary Material for "Long-term changes in lower tropospheric baseline ozone concentrations at northern mid-latitudes"

Section S1. Linear and quadratic regressions for eleven data sets analyzed. The following figures show the results of linear (solid lines) and quadratic (dotted lines) least squares regressions to the seasonal averages of the eleven data sets considered in this work. The data set and the parameters with 95% confidence limits of the respective fits are indicated in each figure.
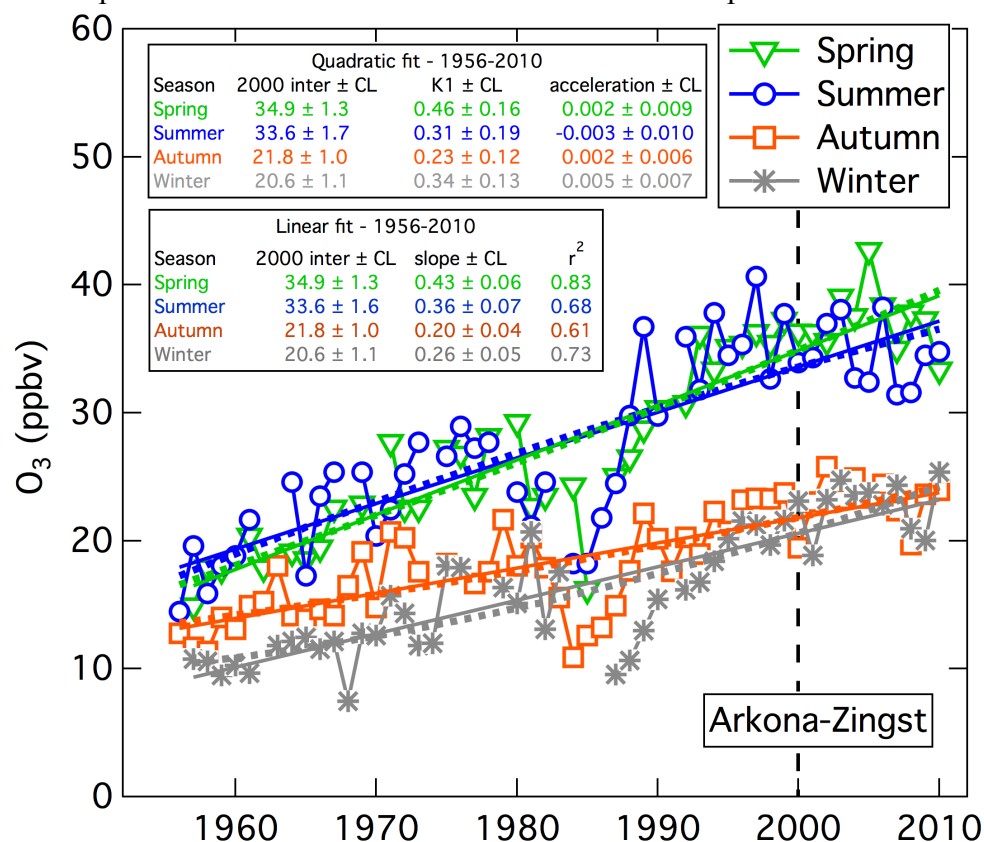

Figure S1. Results for the Arkona-Zingst data set. Figure is generally in the format of Fig. 2 of the text. A linear regression limited to the period before 2000 yields statistically identical parameters as those annotated here. The relative dip in O_3 seen in all seasons in the 1980s is not understood, but the exclusion of those data have little influence on the derived linear regression parameters. The coefficients of the second order terms (acceleration) in the quadratic fits shown here are not significant. It is possible to select portions of the records beginning in the 1980s that do yield statistically significant second order coefficients; however, such fits are not physically reasonable as they predict concentrations much below those observed before 1980. Linear fits are taken as the best simple description of the O_3 changes observed in this measurement record. Seasonal averages were calculated from 1) hourly data obtained from the EMEP data archive for the 1991-2010 Zingst data and 2) from monthly average data from Arkona derived as described by Volz and Kley [1988] and provided by Andreas Volz-Thomas.
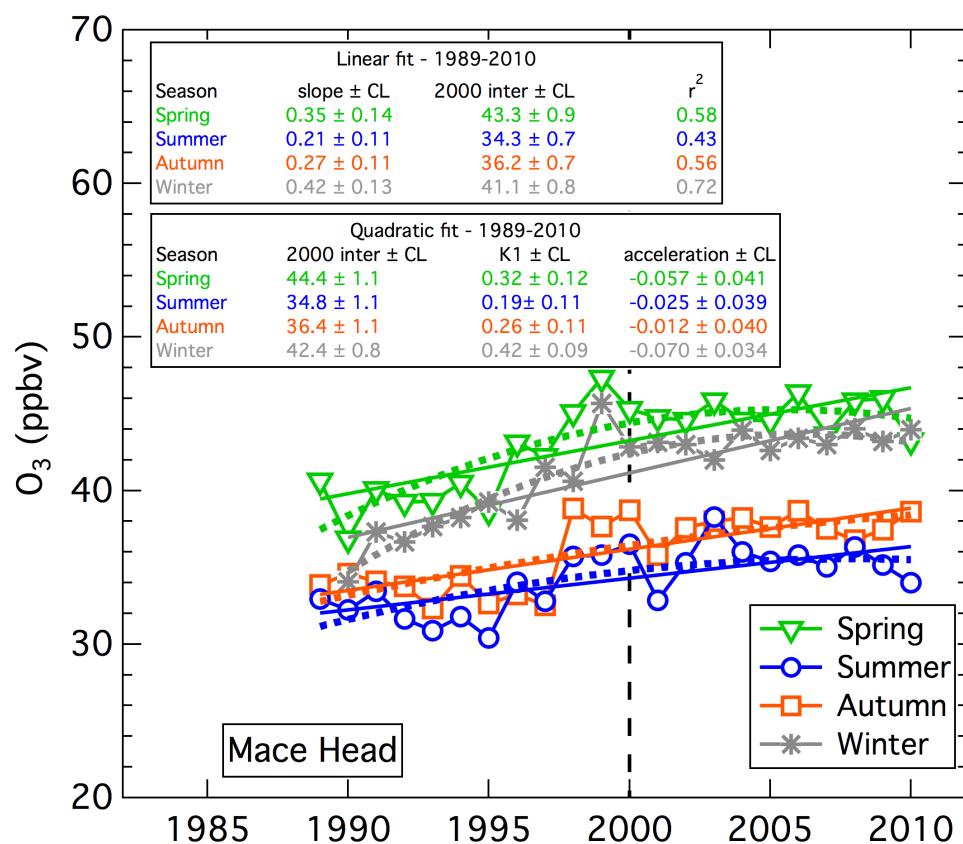
Figure S2. Results for the Mace Head data set. The figure is generally identical to the upper panel of Fig. 3 in the text, where further details of the regressions are discussed. The data set considered here includes the baseline selected data as described in the text, and begins in 1989. *Derwent et al.* [2007] report data as early as 1987, which were baseline selected by somewhat different methods; inclusion of those earlier data with those here do not significantly change either of the regressions in any of the seasons. Seasonal averages were calculated from the monthly average data described by *Derwent et al.* [2007] with later data provided by Richard Derwent.
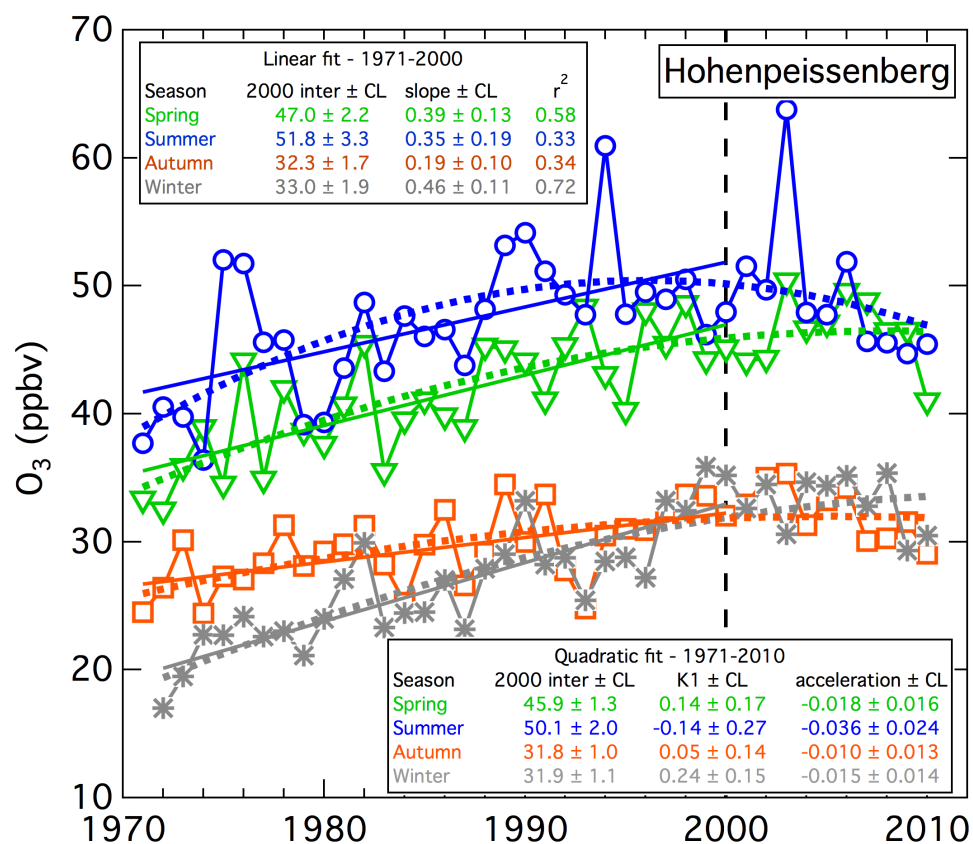
Figure S3. Results for the Hohenpeisenberg data set. The figure is generally identical to Fig. 2 of the text, where details of the regressions are discussed. Seasonal averages were calculated from the monthly average data described by *Gilge et al.* [2010].
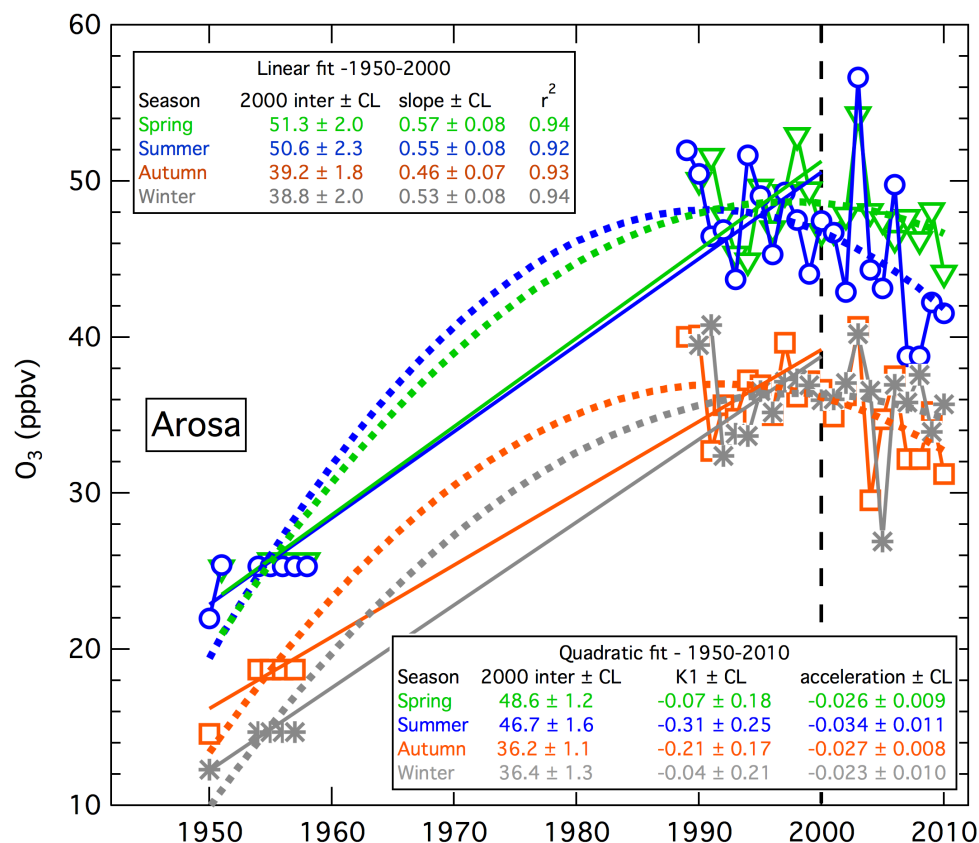
Figure S4. Results for the Arosa data set. Figure is generally in the format of Fig. 2 of the text. The data record includes recent (1989-2010) data combined with earlier data discussed by *Staehelin et al.* [1994]. The 1950-51 seasonal averages were calculated from tabulated diurnal averages. The only data record that survives for the 1954-1958 measurements are averages over all years for a given month; hence those data are duplicated over the respective years. The 1989-2010 seasonal averages were calculated from hourly average data. Here the quadratic fit includes all data; quadratic fits to 1989-2010 (not shown) give similar values for the acceleration, and agree within their confidence limits.
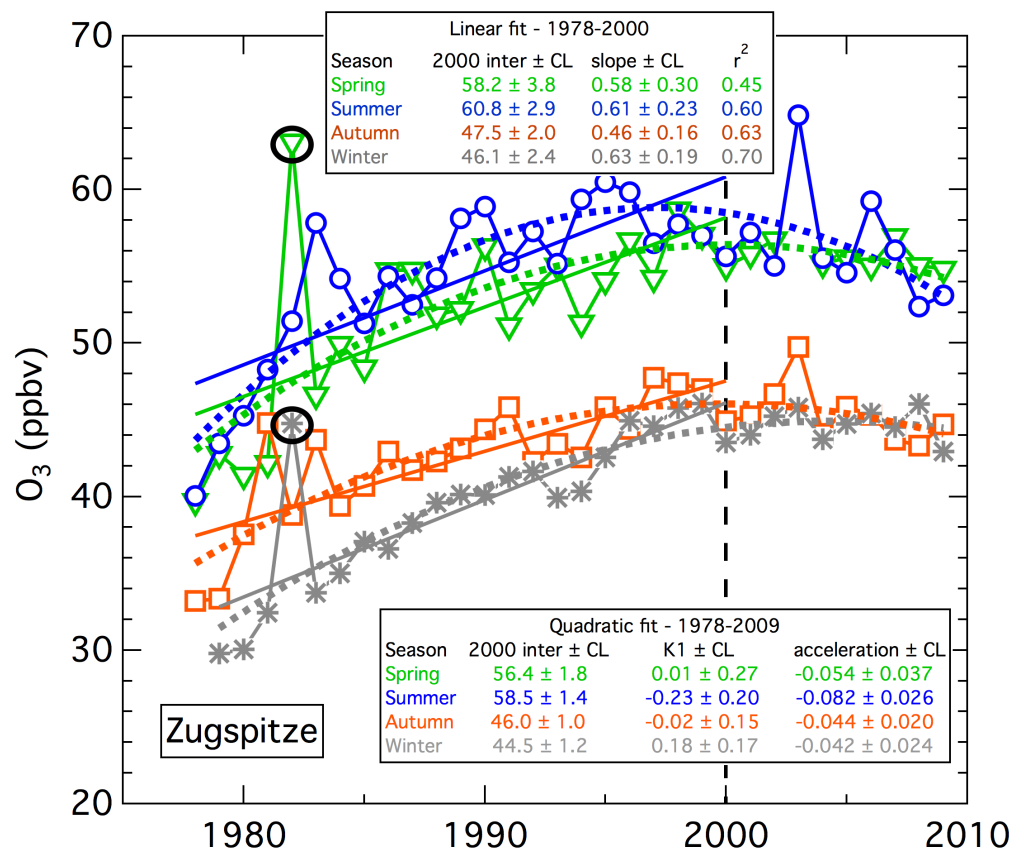
Linear fit - 1978-2000

Season	2000 inter ± CL	slope ± CL	r^2
Spring	58.2 ± 3.8	0.58 ± 0.30	0.45
Summer	60.8 ± 2.9	0.61 ± 0.23	0.60
Autumn	47.5 ± 2.0	0.46 ± 0.16	0.63
Winter	46.1 ± 2.4	0.63 ± 0.19	0.70

Quadratic fit - 1978-2009

Season	2000 inter ± CL	K1 ± CL	acceleration ± CL
Spring	56.4 ± 1.8	0.01 ± 0.27	-0.054 ± 0.037
Summer	58.5 ± 1.4	-0.23 ± 0.20	-0.082 ± 0.026
Autumn	46.0 ± 1.0	-0.02 ± 0.15	-0.044 ± 0.020
Winter	44.5 ± 1.2	0.18 ± 0.17	-0.042 ± 0.024

Zugspitze

Figure S5. Results for the Zugspitze data set. Figure is generally in the format of Fig. 2 of the text. Seasonal averages were calculated from the monthly average data provided by H.-E. Scheel at IMK-IFU, and are as described by *Gilge et al.* [2010]. All data are included in the fits. In the analysis of *Logan et al.* [2012], they excluded January-May 1982 data when computing trends. Exclusion of those data here (the two points indicated by black circles) give regressions with parameters that agree with those shown within in the indicated confidence limits.
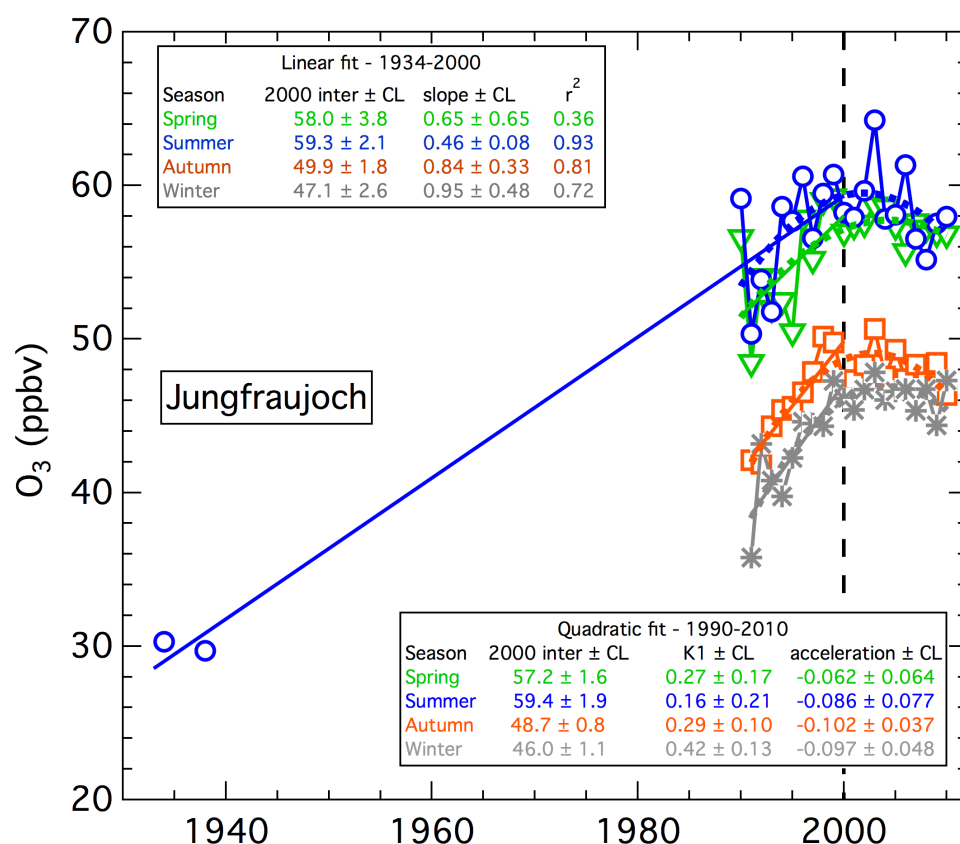
Figure S6. Results for the Jungfraujoch data set. Figure is generally in the format of Fig. 2 of the text. The data record includes recent (1990-2010) data combined with some limited data from the 1930s [*Crutzen,* 1988; Staehelin et al., 1994]; . The 1990-2010 seasonal averages were calculated from the monthly average data provided by Martin Steinbacher, and are as described by *Gilge et al.* [2010]. The linear fit to the 1990-2000 summer data (not shown) gives a slope (0.59 ± 0.66) not statistically significant at the 95% confidence limit; however it is nevertheless consistent with the much more precise slope (0.46 ± 0.08) determined from the data set including the two years from the 1930s. The quadratic fit to the summer data including the 1930s data (not shown) gives an acceleration much less negative (-0.0088 ± 0.0073) than that derived for the past 20 years (-0.086 ± 0.077), although the confidence limit of the latter overlaps with the former.
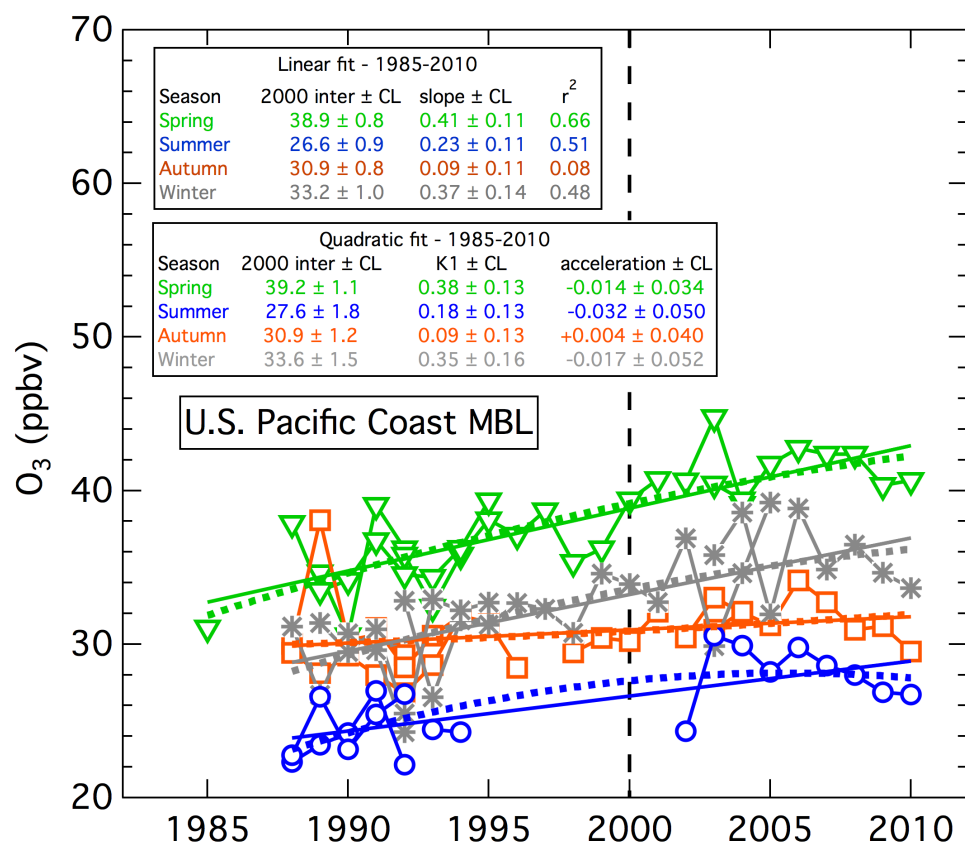
Figure S7. Results for the U.S.Pacific MBL data set. The figure is generally identical to the lower panel of Fig. 3 in the text, where further details of the regressions are discussed. The data set considered here includes baseline selected data [*Parrish et al.,* 2009] as described in the text. The Trinidad Head data were provided by the NOAA Earth System Research Laboratory, Global Monitoring Division (available at http://www.esrl.noaa.gov/gmd/dv/ftpdata.html). Seasonal averages were calculated from hourly average data.
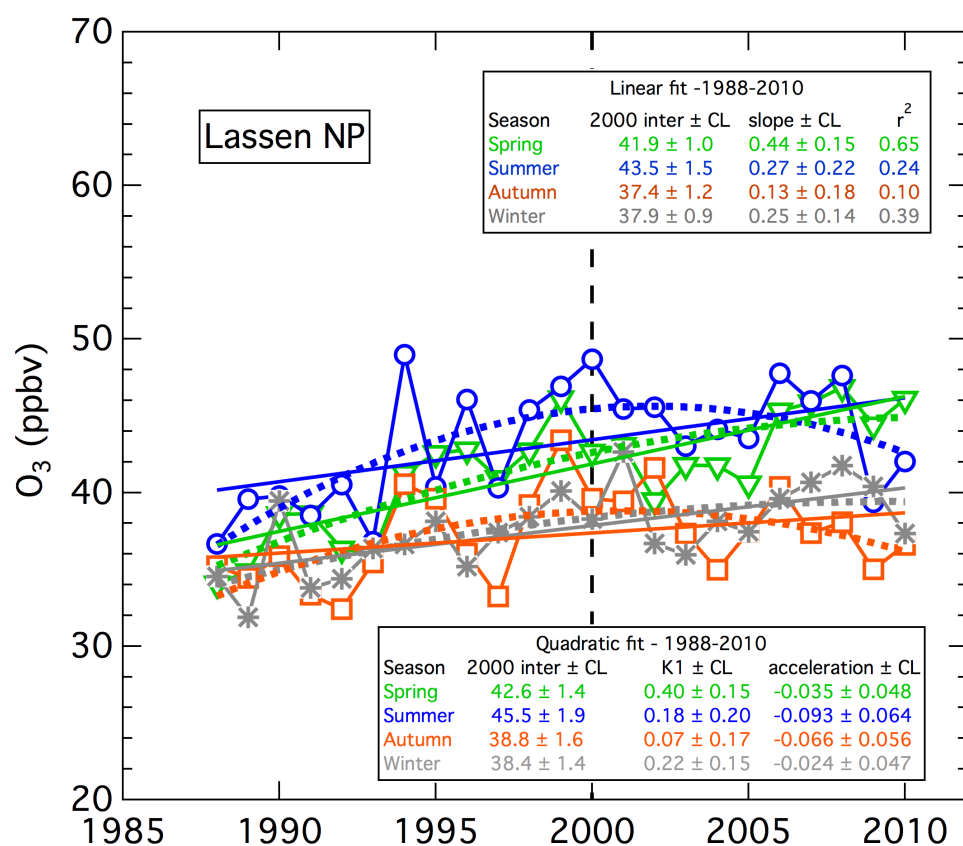
Figure S8. Results for the Lassen NP data set. Figure is generally in the format of Fig. 2 of the text. Similar to the discussion of the Mace Head data set, the acceleration parameters from the quadratic fits are negative in all seasons, and two are statistically significant. Nevertheless, the linear fit includes all years, because the precision of the derived parameters is significantly better, and the data near 2000 appear anomalously high. Except in summer, the slopes and intercepts reported here are in statistical agreement with those reported by *Jaffe et al.* [2003] for the full data sets from 1988-2002. Seasonal trends were calculated from hourly average data provided by the U.S. National Park Service, Air Resources Division (available at http://www.nature.nps.gov/air/monitoring/network.cfm).
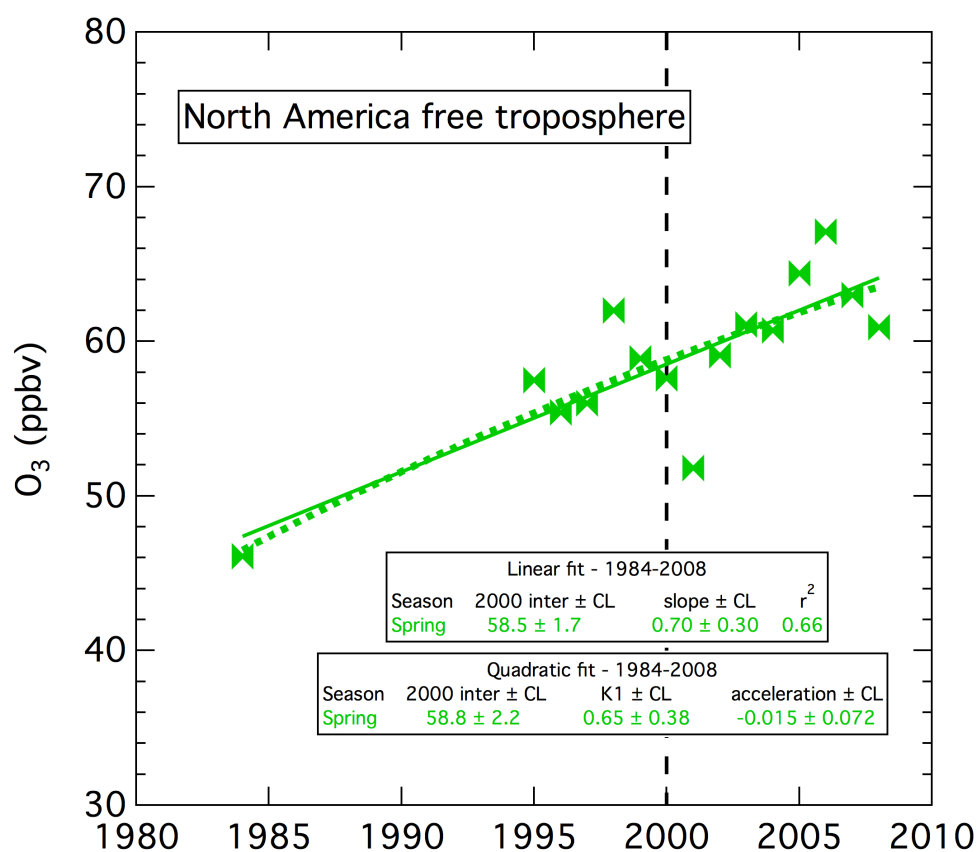
Figure S9. Results for the North American free troposphere data set. Figure is generally in the format of Fig. 2 of the text. The data are those reported by *Cooper et al.* [2010]. As discussed in that reference, exclusion of the 1984 data point does not significantly change the derived parameters, although the confidence limits are then larger.
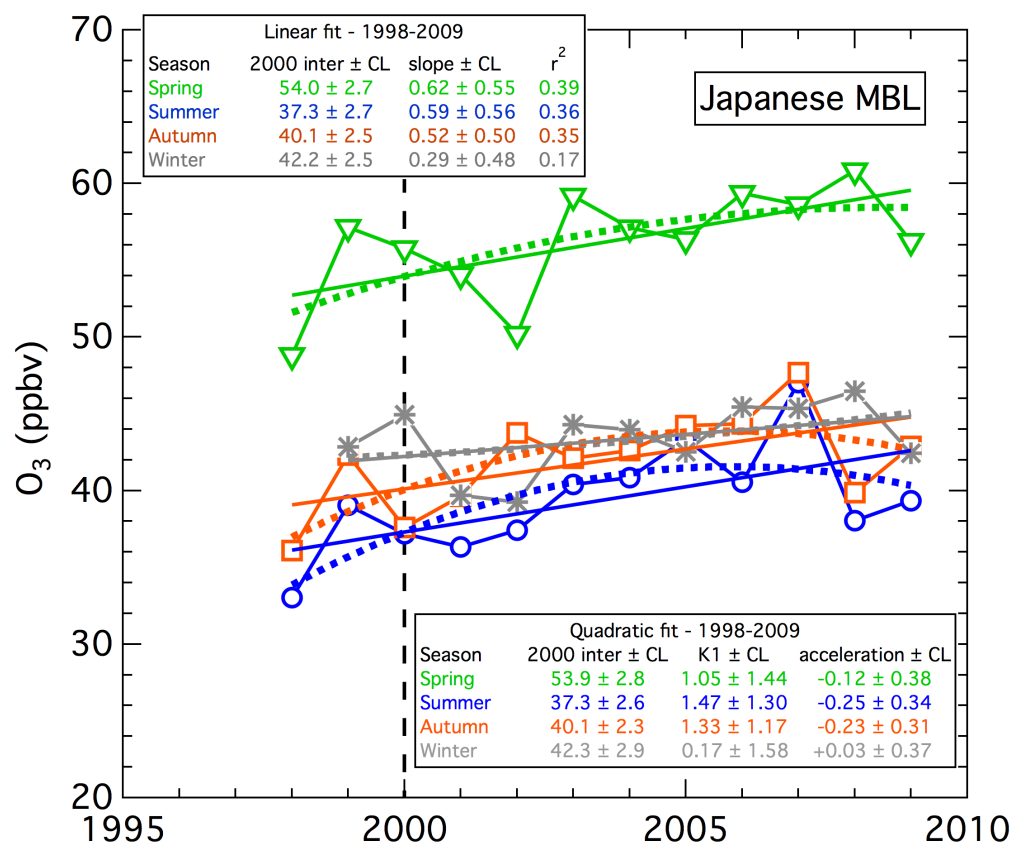
Figure S10. Results for the Japanese MBL data set. The figure is generally in the format of Fig. 2 in the text. The data set is constructed from measurements at three sites as described in the text. Data through 2007 are from *Tanimoto et al.* [2009]; 2008-2009 data are provided by Acid Deposition Monitoring Network in East Asia (EANET).
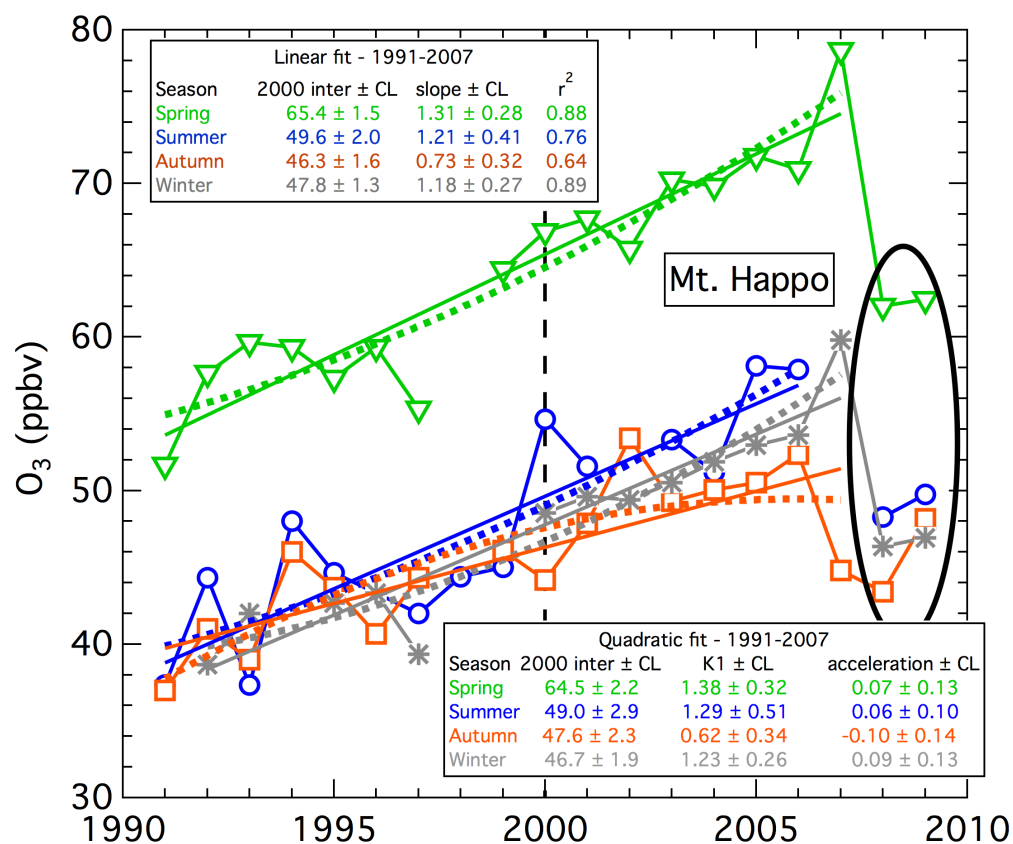
Figure S11. Results for the Mt. Happo data set. The figure is generally in the format of Fig. 2 in the text. The data set through 2007 is taken from *Tanimoto et al.* [2009]. The 2008-2009 data (indicated in oval) are provided by Acid Deposition Monitoring Network in East Asia (EANET), but are not included in the regression fits; see discussion in the text.

Section S2. Comparison of long-term O₃ changes for summer, autumn and winter. The following figures compare the linear and quadratic least squares regressions to the seasonal averages of the eleven data sets for the summer, autumn and winter seasons. Each site is indicated by its own color and symbol. The figures are in the same format as Figs 5 and 6 of the text.

Figure S12. Data and linear and quadratic fits for summer.

Figure S13. Data and linear and quadratic fits for autumn.

Figure S14. Data and linear and quadratic fits for winter.

Section S3. Altitude dependence of 2000 intercepts and average trends for six European sites. The following figures illustrate the elevation dependence of the intercept and slope from the linear least squares regressions for the European sites. The different seasons are color coded with different symbols, and the different sites are labeled.

Fig. S15. Elevation dependence of the year 2000 intercept of the linear regressions to the seasonal averages of the indicated sites (left) and the elevation dependence of the slopes of those linear regressions.

Section S4. Comparisons between baseline selected and unfiltered data sets. The following figures show the results of least squares regressions to the seasonal averages to provide comparisons between baseline selected and unfiltered data sets.

The chart contains the following embedded data tables.

Jungfraujoch – baseline

Linear fit - 1990-2000

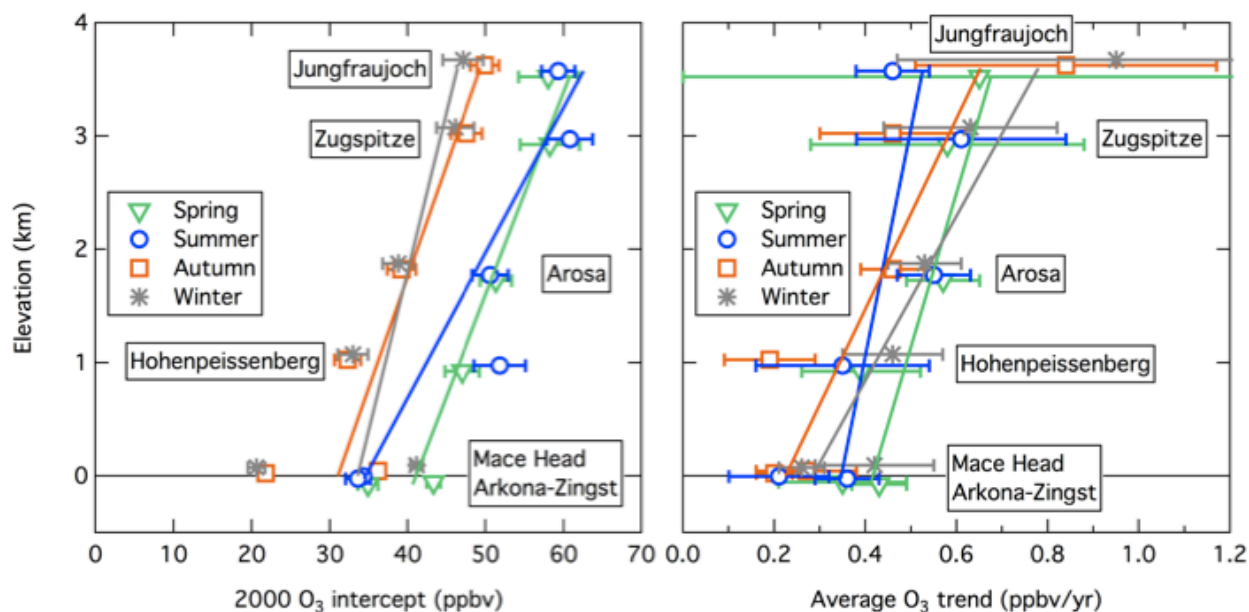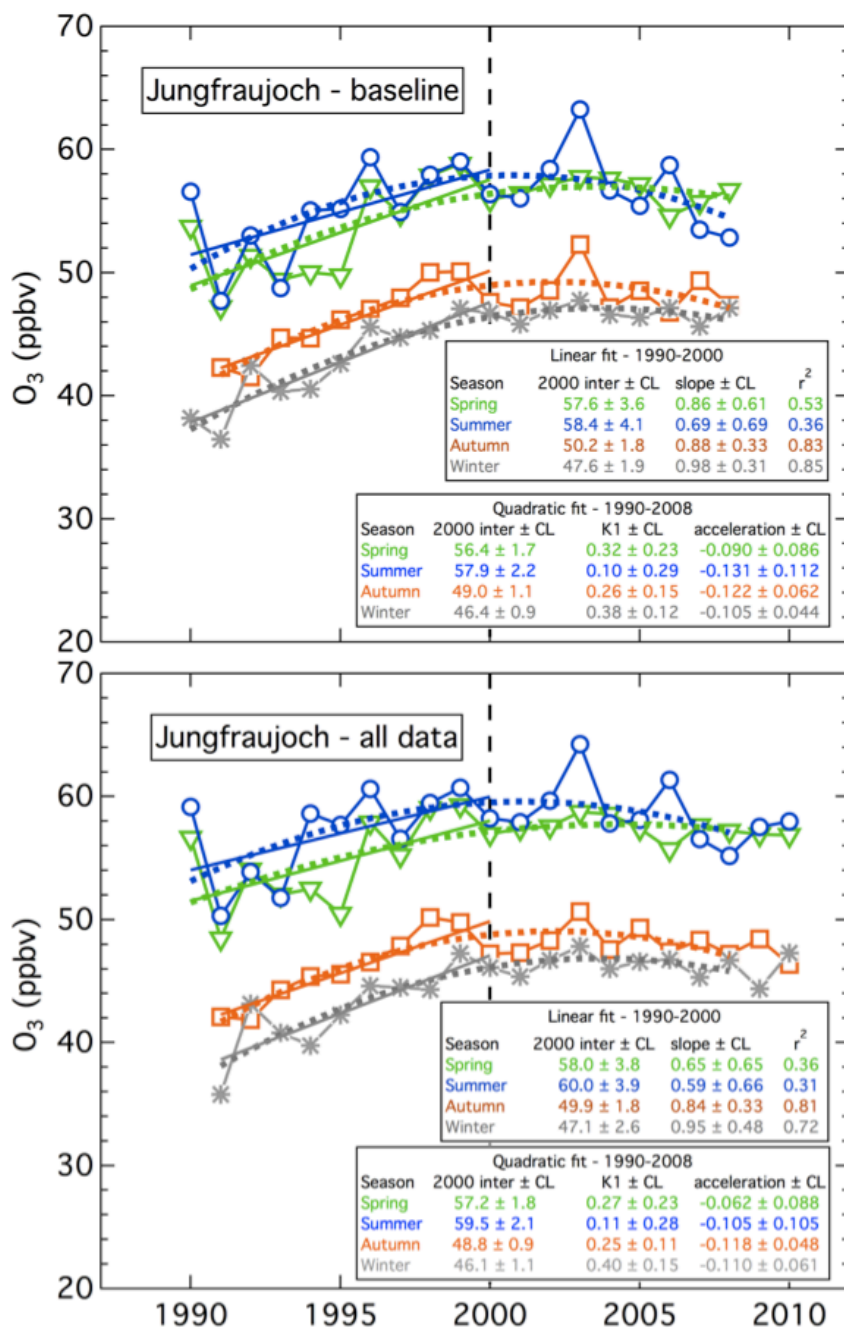| Season	2000 inter ± CL	slope ± CL	r^2
Spring	57.6 ± 3.6	0.86 ± 0.61	0.53
Summer	58.4 ± 4.1	0.69 ± 0.69	0.36
Autumn	50.2 ± 1.8	0.88 ± 0.33	0.83
Winter	47.6 ± 1.9	0.98 ± 0.31	0.85

Quadratic fit - 1990-2008

Season	2000 inter ± CL	K1 ± CL	acceleration ± CL
Spring	56.4 ± 1.7	0.32 ± 0.23	-0.090 ± 0.086
Summer	57.9 ± 2.2	0.10 ± 0.29	-0.131 ± 0.112
Autumn	49.0 ± 1.1	0.26 ± 0.15	-0.122 ± 0.062
Winter	46.4 ± 0.9	0.38 ± 0.12	-0.105 ± 0.044

Jungfraujoch – all data

Linear fit - 1990-2000

Season	2000 inter ± CL	slope ± CL	r^2
Spring	58.0 ± 3.8	0.65 ± 0.65	0.36
Summer	60.0 ± 3.9	0.59 ± 0.66	0.31
Autumn	49.9 ± 1.8	0.84 ± 0.33	0.81
Winter	47.1 ± 2.6	0.95 ± 0.48	0.72

Quadratic fit - 1990-2008

Season	2000 inter ± CL	K1 ± CL	acceleration ± CL
Spring	57.2 ± 1.8	0.27 ± 0.23	-0.062 ± 0.088
Summer	59.5 ± 2.1	0.11 ± 0.28	-0.105 ± 0.105
Autumn	48.8 ± 0.9	0.25 ± 0.11	-0.118 ± 0.048
Winter	46.1 ± 1.1	0.40 ± 0.15	-0.110 ± 0.061

Figure S16. Comparison of the regressions fit to **a)** baseline filtered data and **b)** total data set from Jungfraujoch. The baseline data are only available through 2008, while the total data set extends through 2010.
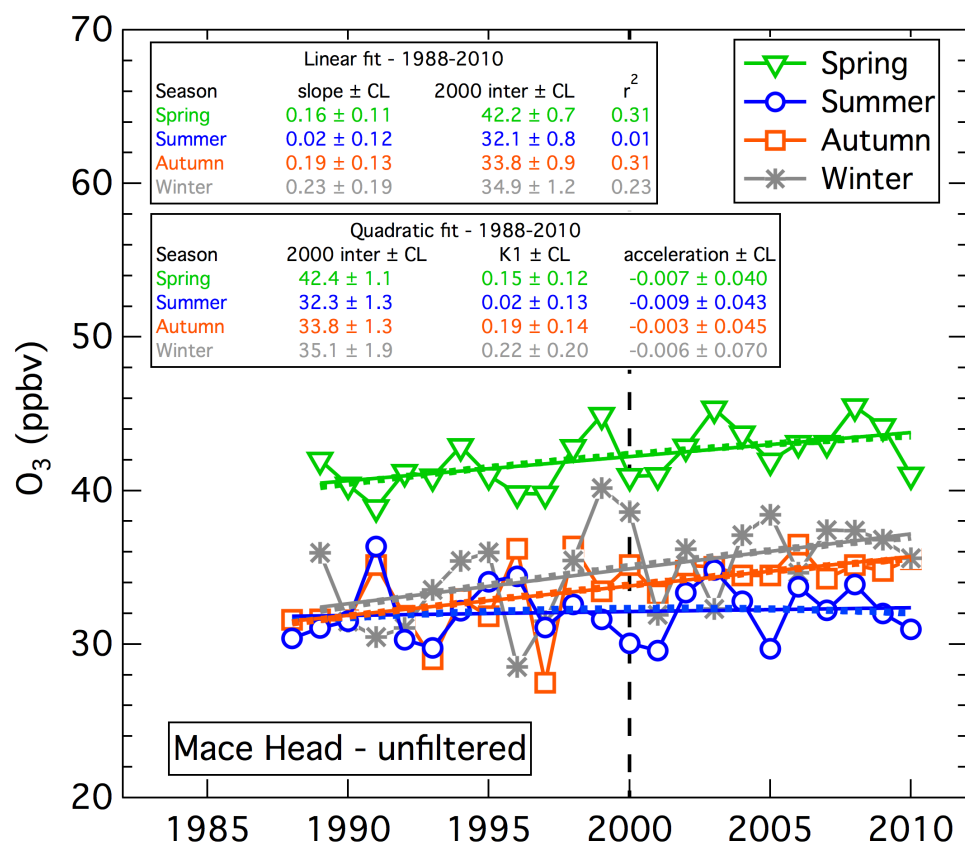
Figure S17. Results of the regressions fit to the total Mace Head data set. The figure is generally in the same format as Fig. S2, except that the data have not been filtered for baseline conditions, and begins in 1988.

Section S5. Linear and quadratic regressions for two sites downwind from North America.
The following figures show the results of linear (solid lines) and quadratic (dotted lines) least squares regressions to the seasonal averages of the complete unfiltered data sets from two sites down wind of North America.
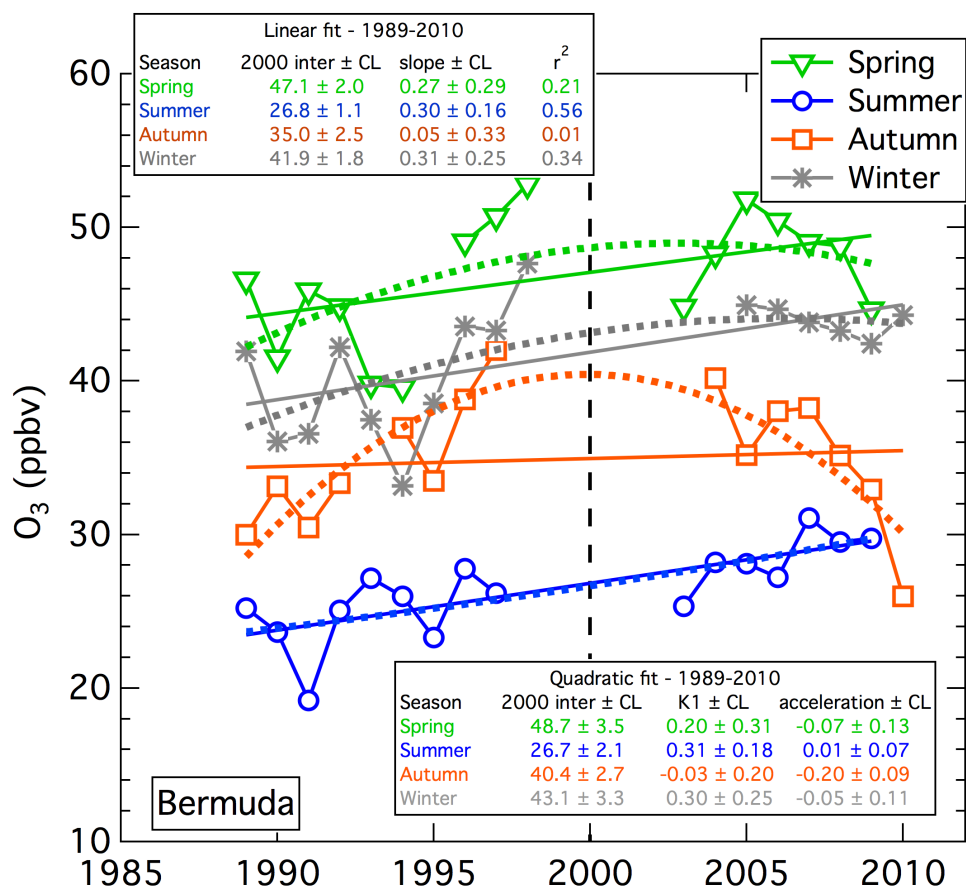

Linear fit - 1989-2010

Season	2000 inter ± CL	slope ± CL	r²
Spring	47.1 ± 2.0	0.27 ± 0.29	0.21
Summer	26.8 ± 1.1	0.30 ± 0.16	0.56
Autumn	35.0 ± 2.5	0.05 ± 0.33	0.01
Winter	41.9 ± 1.8	0.31 ± 0.25	0.34

Quadratic fit - 1989-2010

Season	2000 inter ± CL	K1 ± CL	acceleration ± CL
Spring	48.7 ± 3.5	0.20 ± 0.31	-0.07 ± 0.13
Summer	26.7 ± 2.1	0.31 ± 0.18	0.01 ± 0.07
Autumn	40.4 ± 2.7	-0.03 ± 0.20	-0.20 ± 0.09
Winter	43.1 ± 3.3	0.30 ± 0.25	-0.05 ± 0.11

Bermuda

Figure S18. Results for data collected at Bermuda. The figure is generally in the format of Fig. 2 in the text. The data are from National Oceanic and Atmospheric Administration, Earth System Research Laboratory, Global Monitoring Division.
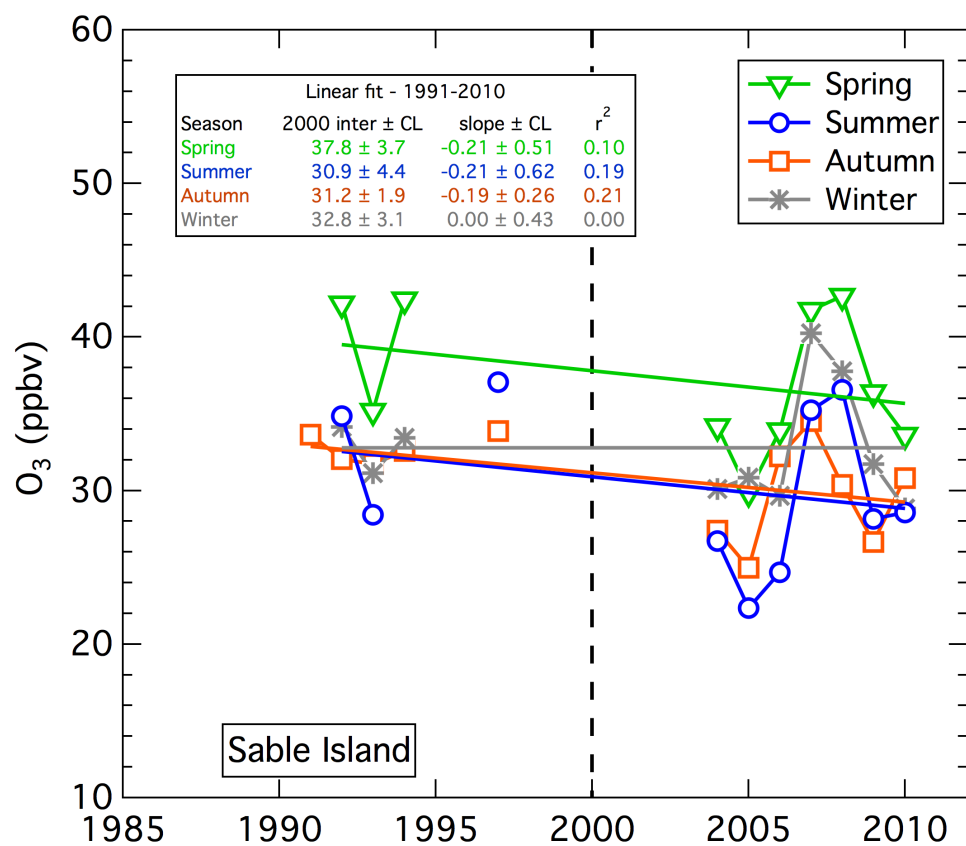
Figure S19. Results for data collected at Sable Island. The figure is generally in the format of Fig. 2 in the text. The data are from *Parrish et al.* [1998] before 2000, and from Nova Scotia Environment, Air Quality and Resource Management Branch after 2000. Since the slopes of the linear regressions are not statistically significant, quadratic fits are not included in this figure.